Inorganic Chemistry

Article

pubs.acs.org/IC

Electronic Stabilization of Trigonal Bipyramidal Clusters: the Role of the Sn(II) Ions in $[Pt_5(CO)_5\{Cl_2Sn(\mu\text{-}OR)SnCl_2\}_3]^{3-}$ (R = H, Me, Et, ^{i}Pr)

Alessandro Ceriotti,[†] Matteo Daghetta,[†] Simona El Afefey,[†] Andrea Ienco,[‡] Giuliano Longoni,[§] Gabriele Manca,[‡] Carlo Mealli,*[,‡] Stefano Zacchini,*[,§] and Salvatore Zarra[§]

[†]Dipartimento di Chimica Inorganica, Metallorganica ed Analitica "Lamberto Malatesta", Università degli Studi di Milano, via Venezian 21, 20133 Milano, Italy

[‡]Istituto di Chimica Composti OrganoMetallici ICCOM-CNR, Via Madonna del Piano 10, 50019 Sesto Fiorentino, Florence, Italy

[§]Dipartimento di Chimica Fisica e Inorganica, Università di Bologna,Viale Risorgimento 4, I-40136, Bologna, Italy

Supporting Information

ABSTRACT: The new $[Pt_5(CO)_5\{Cl_2Sn(\mu\text{-}OR)SnCl_2\}_3]^{3-}$ (R = H, Me, Et, ^{i}Pr; **1**−**4**) clusters contain trigonal bipyramidal (TBP) $Pt_5(CO)_5$ cores, as certified by the X-ray structures of $[Na(CH_3CN)_5][NBu_4]_2$[**1**]·2CH_3CN and $[PPh_4]_3$[**4**]·3CH_3COCH_3. The TBP geometry, which is rare for group 10 metals, is supported by an unprecedented interpenetration with a nonbonded trigonal prism of tin atoms. By capping all the Pt_3 faces, the Sn(II) lone pairs account for both Sn−Pt and Pt−Pt bonding, as indicated by DFT and topological wave function studies. In the TBP interactions, the metals use their vacant s and p orbitals using the electrons provided by Sn atoms, hence mimicking the electronic picture of main group analogues, which obey the Wade's rule. Other metal TBP clusters with the same total electron count (TEC) of 72 are different because the skeletal bonding is largely contributed by d−d interactions (e.g., $[Os_5(CO)_{14}(PR_3)(\mu\text{-}H)_n]^{n-2}$, n = 0, 1, 2). In **1**−**4**, fully occupied d shells at the Pt_{ax} atoms exert a residual nucleophilicity toward the adjacent main group Sn(II) ions permitting their hypervalency through unsual metal donation.

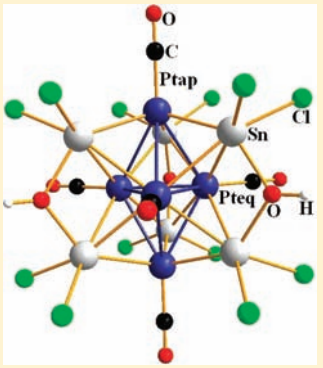

1. INTRODUCTION

Metal carbonyl clusters are of interest in the fields of nanotechnology and catalysis for being a bridge between coordination complexes and metal colloids, particles and surfaces.[1] We have recently reported icosahedral Pt-centered Pt_{13} and Pt_{19} carbonyl clusters, which are decorated on their surfaces by acidic $[Cd_5(\mu\text{-}Br)_5Br_{5-x}(solvent)_x]^{x+}$ rings (solvent = dmf, acetone; x = 2, 3, 4) with a clear relation to thiolate-gold nanoparticles.[2] In fact, while the anionic Pt-carbonyl kernels behave as Lewis bases, the gold species consist of an inner icosahedral or poly icosahedral cation, which is decorated on the surface by $[Au_n(SR)_{n+1}]^-$ (n = 1, 2) staples similar to $R_2P\text{-}(CH_2)_n\text{-}PR_2$ *diphos* chains. To strengthen the analogy, we have reinvestigated the reaction of Pt-carbonyl anions with $SnCl_2$ in excess by isolating formally acidic (following Lewis theory) Pt-carbonyl kernels decorated by $[Cl_2Sn\text{-}(\mu\text{-}OR)\text{-}SnCl_2]^-$ Lewis bases, which are comparable to the mentioned Au-staples. Before this work, the only known Pt-carbonyl cluster containing $SnCl_2$ units was $[Pt_8(SnCl_2)_4(CO)_{10}]^{2-}$.[3]

Here, we report the synthesis and structural characterization of $[Pt_5(CO)_5\{Cl_2Sn(\mu\text{-}OR)SnCl_2\}_3]^{3-}$ clusters (R = H, Me, Et, ^{i}Pr; **1**−**4**), whose ideal D_{3h} model is shown in Scheme 1 (R = H). The system formally consists of an electronically unsaturated $Pt_5(CO)_5$ trigonal bypyramid (TBP), which is capped by six Sn atoms at the vertexes of an ideal trigonal prism. The latter stems from three $\{Cl_2Sn(\mu\text{-}OR)SnCl_2\}^-$ moieties, acting as four-electron donor chelates, similarly to *diphos* ligands.

Scheme 1

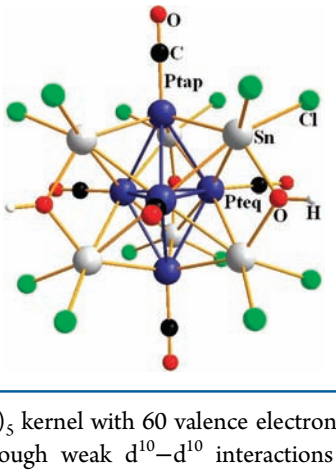

The $Pt_5(CO)_5$ kernel with 60 valence electrons cannot stand alone only through weak d^{10}−d^{10} interactions with possible mixing of the s and p empty Pt orbitals. Therefore, additional electrons are supplied by the six Sn *lone pairs* that cap all the Pt_3 faces (total electron count, TEC = 72). L_5M_5 kernels are rare,[4] and only one example is reported for homoplatinum species, namely the irregular TBP $(PR_3)_5Pt_5H_8$ with TEC = 68.[4e] Eight electrons in the latter are supplied by the six edge-bridging and

Received: July 18, 2011
Published: November 16, 2011

   dx.doi.org/10.1021/ic201519j | *Inorg. Chem.* 2011, 50, 12553−12561

two terminal H atoms. Instead, a regular TBP is found in $Pt_3Re_2(CO)_6(PBu^t_3)_3$ with TEC = 62.[4a,d] The bonding of the latter is evidently supported by d−d interactions involving the d^{10} equatorial Pt atoms and vacant d orbitals of the two L_3Re apical fragments. Persisting electronic unsaturation of $Pt_3Re_2(CO)_6(PBu^t_3)_3$ is shown by the stepwise addition of up to three H_2 molecules with progressive formation of H bridges at adjacent Pt−Re edges, reaching TEC = 68.[4a,d]

The polyhedral skeleton electron pairs theory (PSEPT) for metal TBPs[5] predicts six bonding electron pairs for nine polyhedron edges. Conversely, the effective atomic number rule (EAN),[6] which is an extension of the basic $18e^-$ rule for a single metal suggests nine M−M bonds for a five vertex cluster with TEC = 72, namely, $(18 \times 5 - 72)/2 = 9$. This Article, besides reporting the unprecedented clusters **1**−**4** and two X-ray structures (**1** and **4**), interprets the diverging PSEPT and EAN predictions for M_5 TBP structures emerging from a general analysis of the MO topology.

2. RESULTS AND DISCUSSION

2.1. Synthesis and Characterization of $[Pt_5(CO)_5\{Cl_2Sn(\mu\text{-}OR)SnCl_2\}_3]^{3-}$ (R = H, Me, Et, ^{i}Pr; 1−4). The trianions $[Pt_5(CO)_5\{Cl_2Sn(\mu\text{-}OR)SnCl_2\}_3]^{3-}$ (R = Me, Et, ^{i}Pr; **2**−**4**) were obtained in good yields (55−62% based on Pt) from reactions of $[NBu_4]_2[Pt_{15}(CO)_{30}]$ with $SnCl_2$ (Sn/Pt = 1.2) in CH_3OH (for **2**) or mixtures of ROH/acetone (R = Et, iPr; for **3** and **4**, respectively) in the presence of Na_2CO_3. The role of the base is to eliminate the acidity formed upon deprotonation of the alcohol molecules in accord to eq 1

$$[Pt_{15}(CO)_{30}]^{2-} + 18SnCl_2 + 9ROH \rightarrow 3[Pt_5(CO)_5\{Cl_2Sn(\mu\text{-}OR)SnCl_2\}_3]^{3-} + 7H^+ + H_2 + 15CO \quad (1)$$

The anions **2**−**4** were purified by precipitation with excess $[PPh_4]Cl$ and crystallization from acetone/*n*-hexane or acetone/alcohol. Crystals suitable for X-ray analyses of the salt $[PPh_4]_3[Pt_5(CO)_5\{Cl_2Sn(\mu\text{-}OiPr)SnCl_2\}_3]\cdot 3CH_3COCH_3$ ($[PPh_4]_3[\mathbf{4}]\cdot 3CH_3COCH_3$) were obtained from acetone/Pr^{i}OH. All clusters display very similar ν(CO) [e.g., 2031(s) and 2006(s) cm^{-1} for **2** in acetone]. The μ-OH analogue $[Pt_5(CO)_5\{Cl_2Sn(\mu\text{-}OH)SnCl_2\}_3]^{3-}$ (**1**) has been more conveniently obtained from the reaction of $[NBu_4]_2[Pt_{12}(CO)_{24}]$ with $SnCl_2\cdot 2H_2O$ (Sn/Pt = 1.2) in acetone in the presence of $[NBu_4]Cl$ and Na_2CO_3. Also in this case, the base must neutralize the acidity, which develops according to eq 2.

$$5[Pt_{12}(CO)_{24}]^{2-} + 72SnCl_2 + 36H_2O \rightarrow 12[Pt_5(CO)5\{Cl_2Sn(\mu\text{-}OH)SnCl_2\}_3]^{3-} + 26H^+ + 5H_2 + 60CO \quad (2)$$

The salt of the anion **1**, which was precipitated by addition of isopropanol and recrystallized from CH_3CN/diisopropyl ether, yielded crystals of $[Na(CH_3CN)_5][NBu_4]_2[Pt_5(CO)_5\{Cl_2Sn(\mu\text{-}OH)SnCl_2\}_3]\cdot 2CH_3CN$ suitable for X-ray analysis. The Na^+ ions originate from Na_2CO_3 used as a base. The $[Pt_5(CO)_5\{Cl_2Sn(\mu\text{-}OH)SnCl_2\}_3]^{3-}$ anion displays ν(CO) at 2033(s) and 2006(ms) cm^{-1} in acetone solution.

Compounds **1**−**4** are stable under CO (1 atm), with the coordinated CO ligands slowly exchanging with free carbon monoxide. This allowed the preparation of ^{13}CO-enriched samples of **4** by the stirring of its acetone solution under 1 atm of ^{13}CO for one week. The ^{13}C NMR spectrum in deuterated acetone, which does not change in the temperature range 223−298 K, consists of two nonbinomial triplets at 205.0 ppm ($^1J_{C-Pt}$ = 2539 Hz) and 184.5 ppm ($^1J_{C-Pt}$ = 2621 Hz) with relative intensities 2:3 in agreement with the TBP structure of the $Pt_5(CO)_5$ core of the cluster. Similarly, ^{195}Pt NMR of **4** at 243 K displays two multiplets at δ_{Pt} −4390 and −3949 ppm (relative intensities 2:3), that are attributable to the axial and equatorial Pt-atoms, respectively.

2.2. Structures of $[Pt_5(CO)_5\{Cl_2Sn(\mu\text{-}OR)SnCl_2\}_3]^{3-}$ (R = H, ^{i}Pr; 1, 4). The molecular structures of the anionic clusters $[Pt_5(CO)_5\{Cl_2Sn(\mu\text{-}OR)SnCl_2\}_3]^{3-}$ (R = H, ^{i}Pr; **1**, **4**) have been determined by X-ray crystallography of their $[Na(CH_3CN)_5]$-$[NBu_4]_2[\mathbf{1}]\cdot 2CH_3CN$ and $[PPh_4]_3[\mathbf{4}]\cdot 3CH_3COCH_3$ salts, respectively. Side and top views of **1** and **4** are shown in Figure 1, and their averaged geometric parameters are compared in Table 1 (more details are given the Tables 1S and 2S of the Supporting Information).

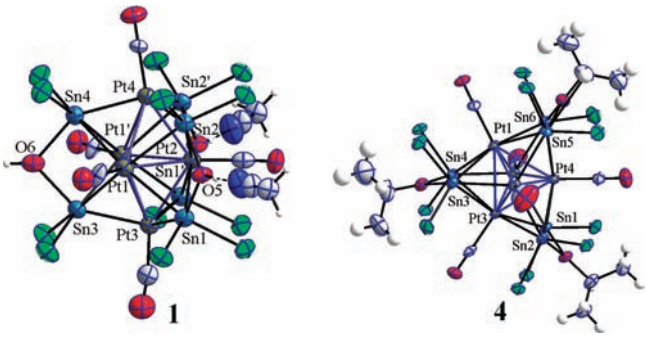

Figure 1. ORTEP drawings (ellipsoids at 50% of probability) of the trianions $[Pt_5(CO)_5\{Cl_2Sn(\mu\text{-}OR)SnCl_2\}_3]^{3-}$, R = H, **1** (side view) and R= ^{i}Pr, **4** (top view). The picture of **1** is built using symmetry operation *x*, 1.5 − *y*, *z*. H-bonding between two of the three OH groups and CH_3CN solvent molecules is highlighted by dashed lines.

Table 1. Selected Bond Distances (Å) in the X-ray Structures of 1 and 4

	$[Pt_5(CO)_5\{Cl_2Sn(\mu\text{-}OH)SnCl_2\}_3]^{3-}$, **1**	$[Pt_5(CO)_5\{Cl_2Sn(\mu\text{-}OPr^i)SnCl_2\}_3]^{3-}$, **4**
Pt_{eq}−Pt_{eq}	2.8387(14)−2.8490(11)	2.8182(6)−2.8477(7)
	av 2.846(2)	av 2.8336(10)
Pt_{ap}−Pt_{eq}	2.8317(15)−2.8918(11)	2.8400(6)−2.8673(5)
	av 2.872(3)	av 2.8570(14)
Pt_{ap}−Sn	2.6541(13)−2.6770(19)	2.6501(7)−2.6716(8)
	av. 2.661(4)	av 2.6603(18)
Pt_{eq}−Sn	2.8084(16)−2.8784(13)	2.7403(7)−2.9092(7)
	av 2.846(5)	av 2.829(2)
Pt_{ap}−C	1.81(3)−1.85(2)	1.858(9)−1.876(8)
	av 1.82(4)	av 1.867(12)
Pt_{eq}-C	1.85(3)−1.874(16)	1.875(8)−1.890(9)
	av 1.87(4)	av 1.882(14)
C−O	1.15(3)−1.18(3)	1.117(12)−1.129(10)
	av 1.16(6)	av 1.12(2)
Sn−O	2.096(11)−2.317(18)	2.136(6)−2.151(5)
	av 2.17(3)	av 2.144(14)
Sn−Cl	2.411(4)−2.449(5)	2.402(2)−2.427(2)
	av 2.425(17)	av 2.416(7)

The $P\bar{1}$ crystals of $[PPh_4]_3[\mathbf{4}]\cdot 3CH_3COCH_3$ contain a **4** cluster anion, three $[PPh_4]^+$ cations and three cocrystallized CH_3COCH_3 molecules in general positions. Conversely, due to

dx.doi.org/10.1021/ic201519j | Inorg. Chem. 2011, 50, 12553−12561

the inner mirror symmetry of the space group $P2_1/m$, the asymmetric unit of $[Na(CH_3CN)_5][NBu_4]_2[\mathbf{1}]\cdot 2CH_3CN$ consists of one-half cluster **1** and one-half $[Na(CH_3CN)_5]^+$ cation, plus an entire $[NBu_4]^+$ cation and one CH_3CN solvent molecule. Both clusters **1** and **4** approach pseudo-D_{3h} symmetry and have a Pt_5 TBP core with a single terminal CO ligand per Pt atom, while the six face-capping Sn atoms from three $Cl_2Sn(\mu\text{-OR})SnCl_2$ moieties form an ideal trigonal prism but remain unbound between themselves (Sn−Sn distances >3.4 Å). A similar TBP structure face-capped by six main group atoms (sulfur) is observed in the redox active species $V_5Cp'_5(\mu_3\text{-}S)_6$ $(Cp' = C_5H_4Me)]^{0,2+}$.[7]

Exact conformation of **1** and **4** to D_{3h} symmetry is likely prevented by crystalline packing effects and H-bonding in **1**. For instance, deviations (<10°) of the Pt_{ax}−CO vectors with respect to the 3-fold axis of the molecule are invariably observed. Moreover, $[Na(CH_3CN)_5][NBu_4]_2[\mathbf{1}]\cdot 2CH_3CN$ presents O−H···N interactions involving only two of the three OH groups with both solvated CH_3CN molecules, thereby giving rise to asymmetrically different Sn−O distances. In particular, the unengaged OH group is less strongly bound to Sn atoms than its analogues [2.317(18) and 2.296(19) Å versus 2.096(11)−2.102(12) Å]. In contrast, the presence of ^{i}Pr substituents instead of H atoms in **4**, is inconsistent with H-bonding, such that all Sn−O distances are equivalent [2.136(6)-2.151(5) Å]. Similar values in the latter narrower range are found in Sn−O(Me)−Sn units bridging between two transition metals (e.g., 2.128(3) Å in $[Bu_4N][Re_2(CO)_8\{Ph_2Sn(\mu\text{-OMe})SnPh_2\}]$[8] or 2.15(2) Å in the isopropoxo-bridged Sn(II) complex $[Me_4N]$-$[\{(Ph_3Sn)_2\{(Ph_2Sn)_2(\mu\text{-O}^i\text{Pr})\}W(CO)_3]$[9]).

In both **1** and **4**, the Pt_{ax}−Sn distances are on the average ∼0.18 Å shorter than the Pt_{eq}−Sn ones for electronic reasons to be later addressed. The average Pt_{ax}−Sn distance of 2.66 Å is longer than a single bond (∼2.55−2.60 Å),[3,10] but ∼0.1 Å shorter than those found in other known cases of a $R_3Sn(II)$ group symmetrically capping a Pt_3 unit (e.g., $(Ph_2PCH_2PPh_2)_3Pt_3(\mu_3\text{-}F_3Sn)(\mu_3\text{-Cl})$[11] or $(Ph_2PCH_2PPh_2)_3Pt_3(\mu_3\text{-}F_3Sn)_2$[12]). The Pt_{eq}−Pt_{eq} and Pt_{ax}−Pt_{eq} distances (∼2.85 Å) are relatively similar and intermediate between a single Pt−Pt bond (∼2.70 Å[13]) and those of 0.66 bond order (∼3.0 Å) found in 44e$^-$ Pt_3 clusters with PR_2 bridges.[14]

The $[Cl_2Sn{-}O(R){-}SnCl_2]^-$ fragment, analogously to a diphosphine ligand, may use the electron pairs of the three-coordinated Sn(II) ions for metal coordination.[15,8] As a matter of fact, a tetra-coordinated (hypervalent) Sn(II) ion can act as donor toward a single metal (Ru[16] or Re[17]) or a Pt_3 face, as found in **1**−**4**. Local pseudo-octahedral geometry is more typical of Sn(IV) species (e.g., the N_4I_2Sn chromophore[18]), whereas an hexacoordinated Sn(II) ion has less symmetric arrangement, as shown by catena-tris$(C_2O_4)_3Sn_2^{2-}$.[19] In **1** and **4**, the Sn is apparently hexa-coordinated and the Sn(II) electrons are important for Pt_5 bonding (vide infra). On the other hand, shorter Pt_{ax}−Sn than Pt_{eq}−Sn distances indicate Pt_{ax} donations, which satisfy the residual acidity of the main group atoms consistently with an uncommon but well documented[20] hypervalency.

2.3. General Electronic Features of TBP Clusters. TBP metal clusters are much less common than tetrahedral ones (∼120 vs 1400 in the Cambridge database[21]), implying a minor electronic stabilization and weaker M−M bonds. Only one-third of the TBP clusters are homometallic and, among them, only three examples of group 10 metals are known, namely, $(PR_3)_5Pt_5H_8$ (TEC = 68),[4] $[Ni_5(CO)_{12}]^{2-}$ (TEC = 76),[22] and $(Ph_3As)_5Pd_5(\mu_3\text{-}SO_2)_2(\mu_2\text{-}SO_2)_2$ (TEC = 72).[23] Conversely, M_4 tetrahedra typically have TEC = 60 and consist of six $2e^-/2c$ M−M bonds, as the number of edges. Nine M−M TBP connectivities do not necessarily imply that, with respect to the PSEPT model, three additional electron pairs participate in skeletal bonding.[5] Importantly, PSEPT is an extension of the Wade rules[24] for main group TBPs such as $B_5H_5^{2-}$[25] (i.e., $n_{vertexes} + 1 = 6$ skeletal electron pairs, which are remarkably the same as in C_4H_4 tetrahedrane). In the M_5 clusters, the metals have generally additional electrons available, which may contribute to skeletal bonding. To verify the point, *ad hoc* MO analyses may help correlating the TBP structures with different TEC values. For instance, the $Pt_3Re_2(CO)_6(PBu^t_3)_3$ compound by Adam has TEC = 62, but its framework can add up to 6 electrons upon stepwise adsorption of three H_2 molecules.[4a,d] While TEC = 72 species are most typical, the d^{10} TBP cluster $[Ni_5(CO)_{12}]^{2-}$[22] has TEC = 76.

Cluster chemists often use also the EAN rule,[6] which predicts nine instead of six M−M bonds for TBP with TEC = 72. Thus, the PSEPT and EAN descriptions are controversial and, since such an electronic situation applies to **1**−**4**, we have performed a DFT analysis of the $[Pt_5(CO)_5\{Cl_2Sn(\mu\text{-OH})SnCl_2\}_3]^{3-}$ model $\mathbf{1}_m$ to validate geometry and correlate wave functions with the M−M bonding features.

2.3(a). DFT Calculations for $[Pt_5(CO)_5\{Cl_2Sn(\mu\text{-OH})SnCl_2\}_3]^{3-}$, $\mathbf{1}_m$. Only the cluster with OH groups was optimized at the B3LYP level,[26] in the gas-phase and without symmetry constraints. Table 2 reports its significant geometric parameters.

Table 2. Optimized Bond Distances (Å) of $[Pt_5(CO)_5\{Cl_2Sn(\mu\text{-OH})SnCl_2\}_3]^{3-}$, $\mathbf{1}_m$ (Experimental Values in Italics)

	range of calculated distances (Å)
Pt_{eq}−Pt_{eq}	2.90−2.92; *(2.84−2.85)*
Pt_{ax}−Pt_{eq}	2.97−3.01; *(2.83−2.89)*
Pt_{ax}−Sn	2.74−2.77; *(2.66)*
Pt_{eq}−Sn	2.93−2.98; *(2.81−2.88)*
Pt_{ax}-C	1.88; *(1.81−1.85)*
Pt_{eq}−C	1.85−1.87; *(1.90)*
C−O	1.15−1.16; *(1.15−1.18)*
Sn−O	2.18−2.19; *(2.10−2.31)*

The optimized Pt−Pt and Pt−Sn distances are somewhat longer than the experimental ones, as expected from the usage of pseudopotentials for the heavier elements.[27] The computed geometry is closer to D_{3h} symmetry than the experimental one, since H-bonding to CH_3CN molecules is not included due to SCF convergence problems. In any case, the calculations afford good reproducibility of the Pt_5 polyhedron stapled by six Sn atoms and average Pt_{ax}−Sn distances, which are about 0.20 Å shorter than the Pt_{eq}−Sn ones (2.75 vs 2.95 Å, respectively). Concerning the Pt−Pt distances, the equatorial ones (2.91 Å) are only 0.05 Å longer than the experimental ones, whereas the Pt_{eq}−Pt_{ax} ones are more overestimated (2.99 vs 2.86 Å). Importantly, all the latter values are significantly larger than a single Pt−Pt bond (∼2.70 Å).[13] For this reason, the Pt_5Sn_6 system is comparable to main group TBPs, such as $B_5H_5^{2-}$, which has six bonding electron pairs over nine edges. In other words, the PSEPT extension of the Wade rule[24,25] to metal clusters seems to be appropriate for these unusual Pt_5 clusters.

dx.doi.org/10.1021/ic201519j | Inorg. Chem. 2011, 50, 12553−12561

2.3(b). Variable Electron Counts in TBP Clusters. In previous studies, we examined the MO architecture of TBP clusters, either formed only by main group elements (e.g., $B_5H_5^{2-}$) or mixed with metals (e.g., M_3S_2 species).[25] In particular, $B_5H_5^{2-}$ had raised divergent opinions about equatorial vs apical redistribution of the skeletal electron pairs.[28,29] Our analysis indicated how, from one σ hybrid and two p_π orbitals per vertex, 15 basic MOs are constructed, of which only six are edge-bonding and populated (see Figure 1 of ref 25). Among mixed M_3S_2 TBPs, numerous $L_xM_3S_2$ structures (x = 2, 3) were rationalized in terms of isolobal analogy[30] and their variable TEC values (47−53), which normally induce loss of either M−S or M−M edge bonding.[25] Remarkably, in some electron rich species, such as $(L_2Cu)_3S_2^{3+}$ with TEC = 50,[31] an unexpected S···S trans-axial interaction was foreshadowed, which has later triggered debate in the literature.[32,33]

With this acquired background on TBP electronic structures, we consider here M_5 metal clusters, starting from the present 72e$^-$ Pt_5Sn_6 systems. The derived wave function topologie are extended to systems with different TECs, as previously done for other M_n species, such as the nido-species M_3[34] and M_4,[35] or closo-M_6 octahedra.[36] For instance, M_6 octahedral clusters are characterized by a general MO framework, which consists of 12 + 12 bonding/antibonding levels, whose energy separations critically affect the bonding features and stability. For TEC = 84, all bonding MOs are populated, allowing as many M-M bonds as the edges. On the other hand, 86e$^-$clusters, which are much more common, have one occupied antibonding MO (formed by d_δ orbitals) at a rather low energy. For any additional electron pairs in the antibonding levels, one M−M bond is lost, while the number of metal lone pairs increases by two units, as conceptually occurs in reducing a bonded H_2 molecule to two separate hydrides. Excess electrons in the octahedral framework may cause alternative effects such as the formation of a *trans*-axial Ni−Ni linkage in the $Cp_6Ni_2Zn_4$ cluster having TEC = 98.[37]

2.3(c). Electron Distribution in $[Pt_5(CO)_5\{Cl_2Sn(\mu\text{-}OR)\text{-}SnCl_2\}_3]^{3-}$. The interaction diagram of Figure 2 highlights the

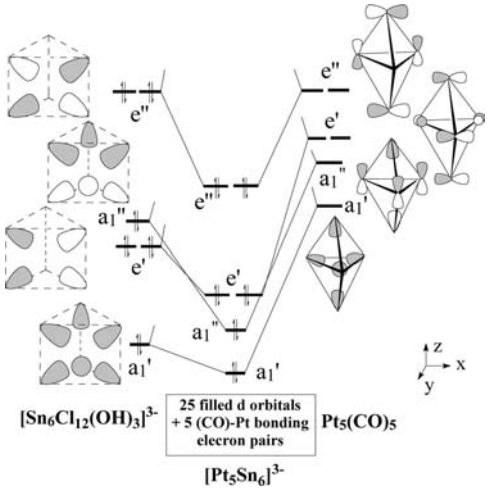

Figure 2. Qualitative MO diagram for the Sn_6−Pt_5 interactions (only one member of the degenerate e sets in D_{3h} symmetry is depicted).

basic interactions, which hold together the Pt_5 and Sn_6 atoms in the D_{3h} model $\mathbf{1_m}$. The Sn(II) lone pairs combine as shown at the left side, while at the right side, the Pt atoms offer one σ hybrid and two pure p orbitals to form the symmetry combinations a_1', a_1'', e′, and e″, which perfectly match the Sn ones. Since the pure s and p Pt orbitals have higher energies, they may be seen as acceptors of the tin electrons, which contribute to partial Pt−Sn bonding but, more importantly, generate Pt−Pt bonds. In fact, the Pt_5Sn_6 MOs of Figure 2 closely recall those of $B_5H_5^{2-}$,[25] the six electron pairs from the Sn(II) allowing Pt_5 skeletal bonding. The diagram in the lower central box indicates the presence of five closed d shells of the (CO)Pt-d^{10} fragments (with some redidual functionality as indicated below) plus the five Pt-CO σ bonding electron pairs.

An additional indication from the MO analysis concerns residual interactions between Pt_{ax} and Sn centers. By neglecting the Pt_{eq} atoms, the local sawhorse geometry around tin (see Scheme 2) corresponds to tetra-coordination of the latter and

Scheme 2. Proposed Bonding Model for Pt_5Sn_6 Clusters to Justify Sn(II) Hypervalency

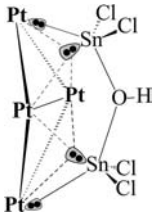

hypervalent $L_4Sn(II)$ units. In other words, each acidic tin atom is surrounded not only by the oxygen and chlorine lone pairs but also a Pt_{ax} one, namely a populated d orbital unused for Pt−Pt bonding. The point is supported by a Mulliken analysis,[38] which indicates all the d populations close to 2e$^-$. Only the two orbitals involved in CO back-donation are slightly less populated (1.8e$^-$) In contrast, much lower populations (∼1.1−1.4 e$^-$) are found in other 72e$^-$ TBPs (e.g., the Os_5 systems discussed below), due to a larger d engagement in M−M bonding. Further evidence of additional Pt_{ax}−Sn bonding is given by ∼0.2 Å shorter distances with respect to the Pt_{eq}−Sn ones as confirmed by the much larger Wiberg indexes[39] (0.60 vs 0.11, respectively). Hypervalency of a main group element through a metal lone pair donation is not so common but examples are reported in the recent literature.[20,40] The achievement of the latter feature, as proposed for **1**−**4**, appears novel.

Scheme 2 summarizes the origin of the Pt−Pt and Pt−Sn bonds in these clusters. The 18 Sn−Pt connections in the drawings of Figure 1 are not all equivalent, as it would be expected if only the six Sn(II) lone pairs were equally shared among all the s and p platinum orbitals, consistently with the PSEPT description. Pt_{ax}→Sn donations are additional bonding components, which confer a multiple bonding character of some sort although no interaction can be classified as 2e$^-$/2c bond.

2.3(d). Nine vs Six M−M Bonds in Other 72e$^-$ TBP Clusters. While PSEPT is the model of reference for the clusters **1**−**4**, other M_5 72e$^-$ TBPs may feature nine M-M bonds consistently with the EAN rule. An example is the hypothetical species $[Os_5(CO)_{15}]^{2-}$ (experimentally unknown but optimized by DFT calculations), which consists of five L_3M-d^8 fragments with one additional electron pair introduced by the doubly negative charge. The experimentally isolated isoelectronic $[Os_5(CO)_{14}(PR_3)(\mu\text{-}H)]^-$[41] and $Os_5(CO)_{15}(\mu\text{-}H)_2$[42] may be formally seen as the result of protonating one or

dx.doi.org/10.1021/ic201519j | Inorg. Chem. 2011, 50, 12553−12561

two Os−Os bonds, without changing the number of electrons, or alternatively two edge-bridging hydrides supply the electrons similarly to the Sn(II) lone pairs in **1**−**4**. At variance with the latter, H_{1s} orbitals are contracted and hardly withstand with a M_3 capping position, an exception being found in $[Pt_3(dppm)_3(\mu_3\text{-}H)]^+$.[43] A detailed MO topological analysis of the latter species is in progress, together with that of other TBPs such as $(PR_3)_5Pt_5H_8$,[4e] $Cp_5Ru_5H_7$,[44] and the Adam's Pt_3Re_2 core with its hydrogenated derivatives $L_9Pt_3Re_2H_x$ (x = 0−6).[4a,d]

The major difference between **1**−**4** and $[Os_5(CO)_{15}]^{2-}$ is due to evident vacancies in the d shells of the latter, which imply direct d-d interactions. Overall, 30 electrons of $[Os_5(CO)_{15}]^{2-}$ are used for Os-CO bonding, while other 30 electrons occupy nonbonding "t_{2g}-like" d orbitals. In principle, the sets of frontier L_3M orbitals (one σ and two d_π per vertex) also form a 15 MOs architecture, with 12 available electrons. This situation approximately reminds those of $B_5H_5^{2-}$ and Pt_5Sn_6 TBPs, with a_1', a_1'', e″, and e′ occupied levels as in Figure 1 of ref 25 or in the present Figure 2. However, a major difference arises from the contraction of the d_π components, which do not ensure sufficient apical/equatorial overlap. This applies, in particular, to the e′ symmetry interactions, formed by in-plane tangential combinations of the d_π orbitals. While the latter ensure two of the three equatorial bonds, equatorial/apical bonding is not feasible and must involve a low lying e′ combination of populated "t_{2g}" d_δ orbitals (e'_{low} in Scheme 3).

Scheme 3. Bonding MO Combinations Contributed to Low Lying d Orbitals

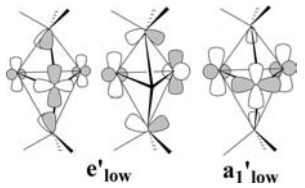

The donations of the latter into the apical d_π orbitals raise the number of skeletal bonds to eight. In a similar manner, an in-phase combination of d_δ orbitals (a'_{1low} in Scheme 3) permits one additional donation into the apical σ hybrids, raising to nine the number of Os−Os bonds, as many as the TBP edges. Hence, the resulting MO architecture consists of 18 rather than 15 MOs with 18 participating electrons. The equatorial d_δ orbitals participate in skeletal bonding a feature that is overlooked by the PSEPT model.

Finally, it is worth mentioning that other neutral TBP Os_5 clusters reach TEC=72 upon coordination of a 16th terminal ligand at one equatorial position, e.g., $L(CO)_{15}Os_5$ (L = CO,[45] $P(CH_3)_3$,[46] $P(O(CH_3))_3$,[47] CNBu^t,[48] *cyclo*-SC_5H_{10},[49] and I[50]). Again, MO analyses confirm the validity of the model with nine Os−Os bonds, as one extra "t_{2g}" filled orbital becomes involved in skeletal bonding, whereas one of the previously considered d_π hybrids preferentially acts as acceptor of the additional ligand (L_4M fragment).

2.3(e). Electron-Rich TBP Clusters. Similarly to M_6 octahedra,[38] a variable TEC may affect M−M bond orders, but not the primary TBP geometry. Among TEC = 76 clusters, an example is $[Rh_5(CO)_{15}]^-$ and congeners, which are complicated by asymmetric distribution of five CO bridges.[51] Since our present interest is mainly for the rare TBPs of group 10 metals, we address in particular the unique 76e$^-$ cluster $[Ni_5(CO)_{12}]^{2-}$, **5**.[22] The latter consists of an equatorial Ni_3 unit with CO bridged edges and two $(CO)_3Ni\text{-}d^{10}$ apical fragments. Closely related is the heteronuclear cluster $[Mo_2Ni_3(CO)_{16}]^{2-}$,[52] with the same Ni_3 equatorial unit but two $L_5Mo\text{-}d^6$ apical fragments, isolobal to the $(CO)_3Ni\text{-}d^{10}$ ones for having one vacant σ hybrid and two populated d_π orbitals. The Mo_2Ni_3 compound was proposed to have five M−M bonds,[52] but the following analysis leads to a different conclusion.

In **5**, the Ni_{eq}−Ni_{ax} distances are much longer than the Ni_{eq}−Ni_{eq} ones (2.78 vs 2.37 Å), as confirmed by previous DFT calculations[53] which did not address the Ni−Ni bond orders. Now, we have optimized the experimentally unknown cluster $[Pt_5(CO)_{12}]^{2-}$, which is more directly relatable to the Pt_5 **1**−**4** TBPs (see the SI). However, very large Pt_{ax}−Pt_{eq} distances of 3.4 Å and the quasi planarity of the apical $(CO)_3Pt$ fragments confirm the fleeing nature of such a species.

The central 44e$^-$ $[(CO)_3Ni_3(\mu\text{-}CO)_3]^{2-}$component of **5** has never been isolated, but 42e$^-$ Pt_3 analogues of formula $Pt_3L_3(\mu\text{-}CO)_3$ (L = phosphine[54]) are well-known to have Pt−Pt single bonds. Remarkably, the two additional electrons in the above Ni_3 dianion do not occupy a M_3 σ^* level (as occurs in 44e$^-$ phosphido-bridged $[Pt_3L_3(\mu\text{-}PR_2)_3]^+$ analogues with 0.66 M−M bond orders[34]) but belong to an in-phase combination of parallel $p_\perp$ orbitals (a_1''), with minor influence on the three σ bonds. The character of the a_1'' HOMO of M_3 CO-bridged dianions (M = Ni, Pt) is at the origin of stacking phenomena upon 2e$^-$ redox processes, which may involve up to ten Pt_3 units to form a wire or cable of metals.[55] Conversely the sequence of redox processes is less extended for the Ni_3 analogue, with no more than three trimers agglomerating in the product $[Ni_3(CO)_3(\mu\text{-}CO)_3]_3^{2-}$.[56] This suggest somewhat different electronic properties of the M_3 building blocks, as also confirmed by subsequent considerations.

There is clear-cut MO evidence that three Ni_{eq}−Ni_{eq} single σ bonds of the central triangle survive also in the TBP **5**, whereas the bond order for Ni_{eq}−Ni_{ax} interactions requires more thoughtful attention. The mentioned $\pi_\perp$ a_1'' HOMO of the central dianion participates in a $Ni_{eq} \rightarrow Ni_{ax}$ donation, which drifts electrons in the σ^* combination of apical and empty σ hybrids (see a_1'' in Scheme 4). Also, the corresponding in-phase

Scheme 4. Ni_{eq}−Ni_{ax} Bonding Interactions in the 76e$^-$ Cluster $[Ni_5(CO)_{12}]^{2-}$ [a]

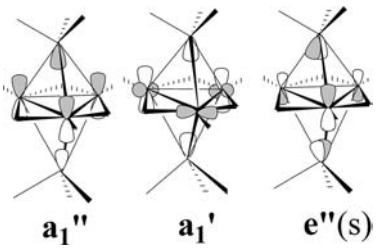

combination of the apical σ hybrids is vacant and engaged in less efficient donation from suitable combination of lower Ni d_δ orbitals, as shown by the MO a_1' in Scheme 4. Finally, the latter shows one member of the degenerate e″ bonding levels, which corresponds to donation from of apical and filled d_π orbitals combinations (out of phase) into equatorial $p_\perp$ ones. Therefore, up to four Ni_{eq}−Ni_{ax} bonds are envisaged, whereas the in-phase e′ combinations of apical d_π apical hybrids (populated) do not

dx.doi.org/10.1021/ic201519j | Inorg. Chem. 2011, 50, 12553–12561

find suitable equatorial acceptors, but are repulsive toward low and populated e′ Ni_3 d_δ orbitals. The latter situation implies four lone pairs in the overall Ni_5 MO architecture, besides four Ni_{ax}−Ni_{eq} bonds.

In summary, the TEC = 76 TBP has in total seven Ni−Ni bonds, as suggested by the EAN rule, that is, $(5 \times 18 - 76)/2 = 7$. The picture contrasts with the five bonds indicated for the $[Mo_2Ni_3(CO)_{16}]^{2-}$ analogue[52] and confirms for TBPs the viewpoint developed for M_6 octahedral clusters.[36] Namely, any electron pair in one antibonding skeletal level cancels one M−M bond, while two lone pairs must be counted in the skeletal architecture.

3. CONCLUSIONS

Compounds **1**−**4** represent a novel class of rare group 10 TBP clusters and raise interesting points about their general electronic structure. The important skeletal bonding is due to the six Sn(II) lone pairs donated to the s and p metal orbitals, thus allowing an electronic picture similar to that of main group TBPs. Accordingly, the PSEPT extension of the Wade rule for metal systems is appropriate in this case. A peculiar role is played by some Pt_{ax} d orbitals, which, being fully populated, exert their nucleophilicity toward the residually acidic Sn(II) ions. The local sawhorse arrangement of the latter (Scheme 2) corresponds to an unusual but not novel[20,40] hypervalency of the main group element attained through metal lone pair donation.

The combined DFT and topological MO[57] studies of Pt_5Sn_6 have been extended to other TBP species to assess the applicability of typical rules for metal clusters, such as PSEPT or EAN, which attempt to interpret skeletal bonding from TEC values. Contradictory results have been found from the different 72e$^-$ TBPs considered in this paper. While PSEPT appropriately accounts for six M−M bonding electron pairs in **1**−**4**, other TEC = 72 clusters are proved to feature nine M−M bonds in agreement with EAN rule (e.g., Os_5 clusters[41,42]). The MO analysis points out that a basic difference between the two cases is the actual degree of involvement of d orbitals in skeletal bonding. The contribution of the latter permits a more complex MO architecture consisting of 18 rather than 15 MO levels. Thus, when the available electrons populate only the bonding set, the number of M−M bonds matches that of the edges (9). On the other hand, the architecture may host additional electrons in the antibonding levels, while maintaining the primary TBP geometry, so that M−M bond weakening (reduced bond order) occurs. An example is that of the Ni_5 cluster **5**, with TEC = 76, which features seven Ni−Ni bonds because four electrons are located in Ni_5 antibonding levels. In summary, a precise description of the bonding in complex clusters requires a more detailed knowledge than that based only on single magic numbers. In particular, the distribution of the key bonding and antibonding levels and their population is fundamental. The validity of the approach for M_6 octahedral clusters[38] is nicely confirmed for TBP compounds.

4. EXPERIMENTAL SECTION

4.1. General Procedures. All reactions and sample manipulations were carried out using standard Schlenk techniques under nitrogen and in dried solvents. All reagents were commercial products (Aldrich) of the highest purity available and used as received, except for $[NR_4]_2[Pt_{3n}(CO)_{6n}]$ (n = 4, 5) which have been prepared according to the literature.[55] Analysis of the Sn and Pt elements were performed by atomic absorption on a Pye-Unicam instrument. C, H, N analysis were carried out on a ThermoQuest FlashEA 1112NC instrument. IR spectra were recorded on a Perkin-Elmer SpectrumOne interferometer in CaF_2 cells. All NMR measurements were performed on Varian Mercury Plus 400 instruments. Structure drawings have been performed with SCHAKAL99.[58]

4.2. Synthesis of $[Na(CH_3CN)_5][NBu_4]_2[Pt_5(CO)_5\{Cl_2Sn(\mu\text{-}OH)SnCl_2\}_3]\cdot 2CH_3CN$. $[NBu_4]Cl$ (0.292 g, 1.05 mmol) and $SnCl_2\cdot 2H_2O$ (0.661 g, 2.93 mmol) were added in solid to a solution of $[NBu_4]_2[Pt_{12}(CO)_{24}]$ (0.681 g, 0.203 mmol) in acetone (30 mL). The solution immediately turned from green to brown-orange and was stirred at room temperature for 4 h. At this stage, the solution displayed a single ν(CO) band at 2048(s) cm^{-1}. Then, Na_2CO_3 (0.115 g, 1.05 mmol) was added and the suspension stirred overnight, until the typical ν(CO) bands of $[Pt_5(CO)_5\{Cl_2Sn(\mu\text{-}OH)SnCl_2\}_3]^{3-}$ appeared at 2033(s) and 2006(ms) cm^{-1}. The crude product was precipitated by addition of isopropanol (50 mL) and recovered by filtration and dried in vacuo. Crystals of $[Na(CH_3CN)_5][NBu_4]_2[Pt_5(CO)_5\{Cl_2Sn(\mu\text{-}OH)SnCl_2\}_3]\cdot 2CH_3CN$ suitable for X-ray analysis were obtained by slow diffusion of *n*-hexane (5 mL) and diisopropyl ether (40 mL) on a solution of the trianion in CH_3CN (20 mL) (yield 0.94 g, 62% based on Pt). The product is soluble in thf, acetone, CH_3CN, and dmf.

$C_{51}H_{96}Cl_{12}N_9Na_1O_8Pt_5Sn_6$ (3099.59): calcd. C 19.74, H 3.12, N 4.07, Sn 23.21, Pt 31.45; found C 19.86, H 3.25, N 3.94, Sn 23.47, Pt 31.54. IR (acetone, 293 K) ν(CO): 2033(s) and 2006(ms) cm^{-1}.

4.3. Synthesis of $[PPh_4]_3[Pt_5(CO)_5\{Cl_2Sn(\mu\text{-}OMe)SnCl_2\}_3]$. Anhydrous $SnCl_2$ (0.489 g, 2.58 mmol) was added in solid to a solution of $[NBu_4]_2[Pt_{15}(CO)_{30}]$ (0.604 g, 0.142 mmol) in CH_3OH (75 mL). The solution turned from green to brown-red and it was stirred at room temperature for 1 h. Then Na_2CO_3 (0.100 g, 0.943 mmol) was added. The suspension was stirred at room temperature for additional three hours. This resulted in the precipitation of an unknown species, removed by filtration, which was soluble in acetone with a single carbonyl stretching band at 2066 cm^{-1}. To the filtrate solution an excess of $[PPh_4]Cl$ (0,503 g) was added, allowing the product to precipitate. After filtration and washing with CH_3OH, the crude product $[PPh_4]_3[Pt_5(CO)_5\{Cl_2Sn(\mu\text{-}OMe)SnCl_2\}_3]$ was recovered by extraction with acetone. Polycrystalline powder was obtained from acetone/methanol. (yield 0.76 g, 55% based on Pt). The product is soluble in thf, acetone, CH_3CN and dmf.

$C_{80}H_{66}Cl_{12}O_8P_3Pt_5Sn_6$ (3361.26): calcd. C 28.56, H 1.98, Sn 21.40, Pt 29.00; found C 28.72, H 2.09, Sn 21.58, Pt 29.16. IR (acetone, 293 K) ν(CO): 2034(s), 2008(ms) cm^{-1}.

4.4. Synthesis of $[PPh_4]_2[Pt_5(CO)_5\{Cl_2Sn(\mu\text{-}OEt)SnCl_2\}_3]$. $SnCl_2\cdot 2H_2O$ (0.541 g, 2.86 mmol) was added in solid to a solution of $[NBu_4]_2[Pt_{15}(CO)_{30}]$ (0.672 g, 0.158 mmol) in a mixture of EtOH (40 mL) and acetone (40 mL). The solution was stirred at room temperature for 1 h and, then, Na_2CO_3 (0.150 g, 1.416 mmol) was added, and the resulting suspension stirred at room temperature for 3 h. The solid was removed by filtration and excess $[PPh_4]Cl$ was added to the solution. Complete precipitation of $[PPh_4]_3[Pt_5(CO)_5\{Cl_2Sn(\mu\text{-}OEt)SnCl_2\}_3]$ was obtained after removal of acetone in vacuo. The crude product was crystallized from acetone/*n*-hexane yielding a polycrystalline powder (yield 0.94 g, 58% based on Pt). The product is soluble in thf, acetone, CH_3CN, and dmf.

$C_{83}H_{72}Cl_{12}O_8P_3Pt_5Sn_6$ (3403.31): calcd. C 30.41 H 2.22, Sn 21.95, Pt 29.76; found C 30.25, H 2.09, Sn 22.10, Pt 29.89. IR (acetone, 293 K) ν(CO): 2034(s), 2008(ms) cm^{-1}.

4.5. Synthesis of $[PPh_4]_3[Pt_5(CO)_5\{Cl_2Sn(\mu\text{-}OiPr)SnCl_2\}_3]\cdot 3CH_3COCH_3$. Anhydrous $SnCl_2$ (0.482 g, 2.54 mmol) was added in solid to a solution of $[NBu_4]_2[Pt_{15}(CO)_{30}]$ (0.602 g, 0.142 mmol) in a mixture of iPrOH (40 mL) and acetone (40 mL). The solution was stirred at 60 °C for 1 h, while the solution was turning from green to brown-red and then Na_2CO_3 (0.100 g, 0.943 mmol) was added. The resulting suspension was stirred at room temperature overnight. This resulted in the precipitation of an unknown species which was removed by filtration, presenting a single carbonyl stretching band at 2066 cm^{-1}. To the filtrate solution an excess of $[PPh_4]Cl$ (0.500 g) was added, allowing the product to precipitate. After filtration and washing with iPrOH, the crude product was dried and extracted with

Table 3. Crystal Data and Experimental Details for $[Na(CH_3CN)_5][NBu_4]_2[Pt_5(CO)_5\{Cl_2Sn(\mu\text{-}OH)SnCl_2\}_3]\cdot 2CH_3CN$ and $[PPh_4]_3[Pt_5(CO)_5\{Cl_2Sn(\mu\text{-}OiPr)SnCl_2\}_3]\cdot 3CH_3COCH_3$

	$[Na(CH_3CN)_5][NBu_4]_2[Pt_5(CO)_5\{Cl_2Sn(\mu\text{-}OH)SnCl_2\}_3]\cdot 2CH_3CN$, **1**	$[PPh_4]_3[Pt_5(CO)_5\{Cl_2Sn(\mu\text{-}OiPr)SnCl_2\}_3]\cdot 3CH_3COCH_3$, **4**
formula	$C_{51}H_{96}Cl_{12}N_9NaO_8Pt_5Sn_6$	$C_{95}H_{99}Cl_{12}O_{11}P_3Pt_5Sn_6$
fw	3099.35	3622.64
T, K	100(2)	100(2)
λ, Å	0.71073	0.71073
crystal system	monoclinic	triclinic
space group	$P2_1/m$	$P\bar{1}$
a, Å	14.007 (3)	15.470(2)
b, Å	22.740(5)	15.647(2)
c, Å	14.397(3)	26.540(5)
α, deg	90	97.942(2)
β, deg	91.844(3)	95.258(2)
γ, deg	90	116.882(2)
cell vol, Å^3	4583.3(18)	5588.3(16)
Z	2	2
D_c, g cm^{-3}	2.246	2.153
μ, mm^{-1}	9.600	7.929
$F(000)$	2868	3392
crystal size, mm	0.16 × 0.14 × 0.11	0.19 × 0.16 × 0.12
θ limits, deg	1.42−25.02	1.50−26.00
index ranges	$-16 \le h \le 16$	$-19 \le h \le 19$
	$-27 \le k \le 27$	$-19 \le k \le 19$
	$-17 \le l \le 17$	$-32 \le l \le 32$
reflns collected	42 865	56708
independent reflns	8302 [R_{int} = 0.1028]	21 892 [R_{int} = 0.0507]
completeness to θ	99.9%	99.4%
data/restraints/params	8302/166/448	21829/619/1146
Goodness on fit on F^2	1.047	1.069
R1 ($I > 2\sigma(I)$)	0.0644	0.0456
wR2 (all data)	0.1920	0.1207
largest peak/hole diff., e Å^{-3}	5.652/−2.416	3.471/−2.611

acetone. The product was crystallized from acetone/iPrOH yielding crystals suitable for X-ray analysis of $[PPh_4]_3[Pt_5(CO)_5\{Cl_2Sn(\mu\text{-}OiPr)SnCl_2\}_3]\cdot 3CH_3COCH_3$. (yield 1.1 g, 71% based on Pt). The product is soluble in thf, acetone, CH_3CN, and dmf.

$C_{95}H_{99}Cl_{12}O_{11}P_3Pt_5Sn_6$ (3622.64): calcd. C 31.47, H 2.75, Sn 19.86, Pt 26.91; found C 31.59, H 2.70, Sn 20.05, Pt 26.78. IR (acetone, 293 K) ν(CO): 2033(s), 2008(ms) cm^{-1}.

4.6. X-ray Crystallographic Study. Crystal data and collection details for $[Na(CH_3CN)_5][NBu_4]_2[Pt_5(CO)_5\{Cl_2Sn(\mu\text{-}OH)SnCl_2\}_3]\cdot 2CH_3CN$ and $[PPh_4]_3[Pt_5(CO)_5\{Cl_2Sn(\mu\text{-}OiPr)SnCl_2\}_3]\cdot 3CH_3COCH_3$ are reported in Table 3. The diffraction experiments were carried out on a Bruker APEX II diffractometer equipped with a CCD detector using Mo−K_α radiation. Data were corrected for Lorentz polarization and absorption effects (empirical absorption correction SADABS).[59] Structures were solved by direct methods and refined by full-matrix least-squares based on all data using F^2.[60] Hydrogen atoms were fixed at calculated positions and refined by a riding model. All non-hydrogen atoms were refined with anisotropic displacement parameters, unless otherwise stated.

4.6.1. $[Na(CH_3CN)_5][NBu_4]_2[Pt_5(CO)_5\{Cl_2Sn(\mu\text{-}OH)SnCl_2\}_3]\cdot 2CH_3CN$. The asymmetric unit of the unit cell contains half of cluster anion (located on a m plane), one $[NBu_4]^+$ cation (on a general position), half $[Na(CH_3CN)_5]^+$ cation (on m) and one CH_3CN molecule (on a general position). Similar U restraints (s.u. 0.005) were applied to the C, N and O atoms. Restraints to bond distances were applied as follow (s.u. 0.01): 1.47 Å for C−N and 1.53 Å for C−C in $[NBu_4]^+$. An hydrogen bond exists between O(5)H(5) and N(6) [O(5)−H(5) 0.95 Å; H(5)···N(6) 1.91 Å; O(5)···N(6) 2.86(2) Å; O(5)−H(5)···N(6) 174.4°]. The difference map is not flat presenting the highest peak (5.652) at 0.7520, 0.1872, 0.8399 [1.00 Å from Pt(1)] and deepest hole (−2.416) at 0.7803, 0.1560, 0.8137 [0.84 Å from Pt(1)]. It is very likely that they are ripple effects on Pt and their locations do not correspond to any realistic positions for real atoms. Thus, they have not been included in the model.

4.6.2. $[PPh_4]_3[Pt_5(CO)_5\{Cl_2Sn(\mu\text{-}OiPr)SnCl_2\}_3]\cdot 3CH_3COCH_3$. The asymmetric unit of the unit cell contains one cluster anion, three $[PPh_4]^+$ cations and three CH_3COCH_3 molecules (all on general positions). Similar U restraints (s.u. 0.005) were applied to the C and O atoms. One CH_3COCH_3 molecule is disordered over two positions. Disordered atomic positions were split and refined using one occupancy parameter per disordered group. Restraints to bond distances were applied as follow (s.u. 0.01): 1.21 Å for C−O and 1.51 Å for C−C in CH_3COCH_3.

4.7. Computational Details. The models were optimized at the hybrid density functional theory (DFT) using Becke's three-parameter hybrid exchange-correlation functional,[26a] containing the nonlocal gradient correction of Lee, Yang, and Parr[26b] (B3LYP) within the Gaussian09 program.[61] For all of the fully optimized structures, calculations of vibrational frequencies were performed to confirm their nature as stationary point.

The effective Stuttgart/Dresden core potential (SDD)[62] was adopted for the Pt and Sn atoms with a polarization f function with exponent 0.993 (for Pt) and d function with exponent 0.186 (for Sn) with the associated double-ζ full double-ζ basis functions. The basis set used for the remaining atomic species was the 6-31G, with the important addition of the polarization functions (d, p) for all atoms, including the hydrogens. Qualitative MO arguments have been developed thanks to the EHMO method[63] and the CACAO[57] package with its graphic interface. The coordinates of the optimized structure have been reported in the Supporting Information.

dx.doi.org/10.1021/ic201519j | Inorg. Chem. 2011, 50, 12553−12561

■ ASSOCIATED CONTENT

Supporting Information

CIF files giving X-ray crystallographic data for the structure determinations of $[Na(CH_3CN)_5][NBu_4]_2[Pt_5(CO)_5\{Cl_2Sn(\mu\text{-}OH)SnCl_2\}_3]\cdot 2CH_3CN$ and $[PPh_4]_3[Pt_5(CO)_5\{Cl_2Sn(\mu\text{-}OiPr)SnCl_2\}_3]\cdot 3CH_3COCH_3$, Cartesian coordinates of the optimized compound $[Pt_5(CO)_5(Sn_2Cl_4OH)_3]^{3-}$ ($\mathbf{1_m}$), $[Pt_5(CO)_{12}]^{2-}$, $[Os_5(CO)_{15}]^{2-}$, $[Os_5(CO)_{15}H]^{-}$, and $Os_5(CO)_{15}H_2$, bond lengths [Å] and angles [deg] for the experimental structures of $[Na(CH_3CN)_5][NBu_4]_2[Pt_5(CO)_5\{Cl_2Sn(\mu\text{-}OH)SnCl_2\}_3].2CH_3CN$, **1**, and $[PPh_4]_3[Pt_5(CO)_5\{Cl_2Sn(\mu\text{-}O^iPr)SnCl_2\}_3]\ 3CH_3COCH_3$, **4**, and full reference 61. This material is available free of charge via the Internet at http://pubs.acs.org.

■ AUTHOR INFORMATION

Corresponding Author

*E-mail: stefano.zacchini@unibo.it (S. Z.); carlo.mealli@iccom.cnr.it (C. M.).

■ ACKNOWLEDGMENTS

This work was supported by the Ministero dell'Istruzione, Università e Ricerca (MIUR), project PRIN2008 No. 2008RFEB3X. The authors (A.I., G.M., C.M.) acknowledge the ISCRA-CINECA HP grant "HP10BNL89W". We whish to thank the Referees for useful suggestions and comments.

■ REFERENCES

(1) (a) Gates, B. C. *Chem. Rev.* **1995**, *95*, 511. (b) Lewis, L. N. *Chem. Rev.* **1993**, *93*, 2693. (c) Alexeev, O. S.; Gates, B. C. *Ind. Eng. Chem. Res.* **2003**, *42*, 1571. (d) Braunstein, P., Oro, L. A., P. Raithby, R., Eds. *Metal Clusters in Chemistry*; Wiley-VCH: Weinheim, Germany, 1999, Vol. 2. (e) Ishiguro, A.; Liu, Y.; Nakajima, T.; Wakatsuki, Y. *J. Catal.* **2002**, *206*, 159. (f) Alexeev, O.; Panjabi, G.; Gates, B. C. *J. Catal.* **1998**, *173*, 196. (g) Femoni, C.; Kaswalder, F.; Iapalucci, M. C.; Longoni, G.; Zacchini, S. *Coord. Chem. Rev.* **2006**, *250*, 1580.

(2) Femoni, C.; Iapalucci, M. C.; Longoni, G.; Zacchini, S.; Zarra, S. *J. Am. Chem. Soc.* **2011**, *133*, 2406.

(3) Brivio, E.; Ceriotti, A.; Garlaschelli, L.; Manassero, M.; Sansoni, M. *J. Chem. Soc., Chem. Commun.* **1995**, 2055.

(4) (a) Adams, R. D.; Captain, B.; Beddie, C.; Hall, M. B. *J. Am. Chem. Soc.* **2007**, *129*, 986. (b) Brayshaw, S. K.; Ingleson, M. J.; Green, J. C.; McIndoe, J. S.; Raithby, P. R.; Kociok-Kohn, G.; Weller, A. S. *J. Am. Chem. Soc.* **2006**, *128*, 6247. (c) Smidt, S. P.; Pfaltz, A.; Martinez-Viviente, E.; Pregosin, P. S.; Albinati, A. *Organometallics* **2003**, *22*, 1000. (d) Adams, R. D.; Captain, B. *Angew. Chem., Int. Ed.* **2007**, *46*, 2. (e) Gregson, D.; Howard, J. A. K.; Murray, M.; Spencer, J. L. *J. Chem. Soc., Chem. Commun.* **1981**, 716.

(5) (a) Mingos, D. M. P. *Nature Phys. Sci. (London)* **1972**, *236*, 99. (b) Mingos, D. M. P. *Acc. Chem. Res.* **1984**, *17*, 311.

(6) (a) Sidgwick, N. V. *Trans. Faraday Soc.* **1923**, *19*, 469. (b) Sidgwick, N. V. *The Electronic Theory of Valency*; Clarendon Press: Oxford, U.K., 1927; Chapter 10. (c) Kharas, K. C. C.; Dahl, L. F. *Adv. Chem. Phys.* **1988**, *70*, 1. (d) Owen, S. M. *Polyhedron* **1988**, *7*, 253. (e) Mingos, D. M. P.; Johnson, R. L. *Struct. Bonding (Berlin)* **1987**, *68*, 29.

(7) (a) Eremenko, I. L.; Katugin, A. S.; Pasynskii, A. A.; Struchkov, Yu. T.; Shklover, V. E. *J. Organomet. Chem.* **1988**, *345*, 79. (b) Bolinger, C. M.; Darkwa, J.; Gammie, G.; Gammon, S. D.; Lyding, J. W.; Rauchfuss, T. B.; S.R.Wilson, S. R. *Organometallics* **1986**, *5*, 2386.

(8) Adams, R. D.; Captain, B.; Hollandsworth, C. B.; Johansson, M.; Smith Junior, J. L. *Organometallics* **2006**, *25*, 3848.

(9) Rochfort, G. L.; Ellis, J. E. *J. Organomet. Chem.* **1983**, *250*, 277.

(10) Spivak, G. J.; Hao, L.; Vittal, J. J.; Puddephatt, R. J. *J. Am. Chem. Soc.* **1996**, *118*, 225.

(11) Douglas, G.; Jennings, M. C.; Manijlovic-Muir, L.; Muir, K. W.; Puddephatt, R. J. *Chem. Commun.* **1989**, 159.

(12) Jennings, M. C.; Schoettel, G.; Roy, S.; Puddephatt, R. J.; Douglas, G.; Manojlovic-Muir, L.; Muir, K. W. *Organometallics* **1991**, *10*, 580.

(13) (a) Cittadini, V.; Leoni, P.; Marchetti, L.; Pasquali, M.; Albinati, A. *Inorg. Chim. Acta* **2002**, *330*, 25. (b) Calabrese, J. C.; Dahl, L. F.; Chini, P.; Longoni, G.; Martinengo, S. *J. Am. Chem. Soc.* **1974**, *96*, 2616. (c) Braddock-Wilking, J.; Corey, J. Y.; Dill, K.; Rath, N. P. *Organometallics* **2002**, *21*, 5467. (d) Wachtler, H.; Schuh, W.; Ongania, K.-H.; Wurst, K.; Peringer, P. *Organometallics* **1998**, *17*, 5640.

(14) (a) Bender, R.; Braunstein, P.; Dedieu, A.; Ellis, P. D.; Huggins, B.; Harvey, P. D.; Sappa, E.; Tiripicchio, A. *Inorg. Chem.* **1996**, *35*, 1223. (b) Cavazza, C.; Fabrizi de Biani, F.; Funaioli, T.; Leoni, P.; Marchetti, F.; Marchetti, L.; Zanello, P. *Inorg. Chem.* **2009**, *48*, 1385. (c) Leoni, P.; Marchetti, F.; Pasquali, M.; Marchetti, L.; Albinati, A. *Organometallics* **2002**, *21*, 2176. (d) Fabrizi de Biani, F.; Ienco, A.; Laschi, F.; Leoni, P.; Marchetti, F.; Marchetti, L.; Mealli, C.; Zanello, P. *J. Am. Chem. Soc.* **2005**, *127*, 3076.

(15) Schneider, J. J.; Czap, N.; Hagen, J.; Rust, J.; Kruger, C.; Mason, S. A.; Bau, R.; Ensling, J.; Gutlich, P.; Wrackmeyer, B. *Chem.—Eur. J.* **2000**, *6*, 625.

(16) Albertin, G.; Antoniutti, S.; Bacchi, A.; Pelizzi, G.; Zanardo, G. *Organometallics* **2008**, *27*, 4407.

(17) Albertin, G.; Antoniutti, S.; Castro, J.; Garcia-Fontan, S.; Zanardo, G. *Organometallics* **2007**, *26*, 2918.

(18) Kuchta, M. C.; Parkin, G. *Polyhedron* **1996**, *15*, 4599.

(19) Ayyappan, S.; Cheetham, A. K.; Natarajan, S.; Rao, C. N. R. *Chem. Mater.* **1998**, *10*, 3746.

(20) (a) Hoffmann, R.; Rogachev, A. Yu. Private communication of their work in progress on the subject. (b) *Chemistry of Hypervalent Compounds*; Akiba, K.-y., Ed. ; Wiley, 1999.

(21) *Cambridge Structural Database System, (CSD)*; Cambridge Crystallographic Data Centre: Cambridge, U.K, 2011; http://www.ccdc.cam.ac.uk.

(22) (a) Longoni, G.; Chini, P.; Lower, L. D.; Dahl, L. F. *J. Am. Chem. Soc.* **1975**, *97*, 5034. (b) Petz, W.; Neumuller, B. *Z. Anorg. Allg. Chem.* **2001**, *627*, 2274.

(23) Burrows, A. D.; Mingos, D. M. P.; Powell, H. R. *J. Chem. Soc., Dalton Trans.* **1992**, 261.

(24) (a) Wade, K. *J. Chem. Soc. Chem. Commun.* **1971**, 792. (b) Wade, K. *Adv. Inorg. Radiochem.* **1976**, *18*, 1. (c) O'Neil, M. E.; Wade, K. *Comprehensive Organometallic Chemistry*; Wilkinson, G., Stone, F. G.A., Abel, E., Eds.; Pergamon Press: New York, 1982.

(25) Mealli, C.; Messaoudi, A.; Ienco, A. *Theor. Chem. Acc.* **2009**, *123*, 365.

(26) (a) Becke, A. D. *J. Chem. Phys.* **1993**, *98*, 5648. (b) Lee, C.; Yang, W.; Parr, R. G. *Phys. Rev. B* **1988**, *37*, 785. (c) Vosko, S. H.; Wilk, L.; Nusair, M. *Can. J. Phys.* **1980**, *58*, 1200. (d) Stephens, P. J.; Devlin, F. J.; Chabalowski, C. F.; Frisch, M. J. *J. Phys. Chem.* **1994**, *98*, 11623.

(27) (a) Hirva, P.; Haukka, M.; Jakonen, M.; Moreno, M. A. *J. Mol. Mod.* **2008**, *17*, 171. (b) Lombardi, J. R.; Davis, B. *Chem. Rev.* **2002**, *102*, 2431. (c) Barden, C. J.; Rienstra-Kiracofe, J. C.; Schaefer, H. F. III *J. Chem. Phys.* **2000**, *113*, 690. (d) Yanagisawa, S.; Tsuneda, T.; Hirao, K. *J. Chem. Phys.* **2000**, *112*, 545.

(28) von Ragué Schleyer, P.; Subramanian, G.; Dransfeld, A. *J. Am. Chem. Soc.* **1996**, *118*, 9988.

(29) Burdett, J. K.; Eisenstein, O. *J. Am. Chem. Soc.* **1995**, *117*, 939.

(30) Hoffmann, R. Building Bridges Between Inorganic and Organic Chemistry, Nobel lecture, 8 December 1981.

(31) Mealli, C.; Ienco, A.; Poduska, A.; Hoffmann, R. *Angew. Chem., Int. Ed.* **2008**, *47*, 1 and references therein.

(32) (a) Alvarez, S.; Hoffmann, R.; Mealli, C. *Chem.—Eur. J.* **2009**, *15*, 8358. (b) Sherer, E. C.; Kinsinger, C. R.; Kormos, B. L.; Thompson, J. D.; Cramer, C. J. *Angew. Chem., Int. Ed.* **2002**, *41*, 1953.

(33) (a) Berry, J. F. *Chem.—Eur. J.* **2010**, *16*, 2719. (b) Alvarez, S.; Ruiz, E. *Chem.—Eur. J.* **2010**, *16*, 2726. (c) Mealli, C.; Messaoudi, A.; Ienco, A. manuscript in preparation.

(34) Mealli, C. *J. Am. Chem. Soc.* **1985**, *107*, 2245.
(35) Mealli, C.; Proserpio, D. M. *J. Am. Chem. Soc.* **1990**, *112*, 5884.
(36) Mealli, C.; López, J. A.; Sun, Y.; Calhorda, M. J. *Inorg. Chim. Acta* **1993**, *213*, 199.
(37) Budzelaar, P. H. M.; Boersma, J.; M.van der Kerk, G. J.; Spek, A. L.; Duisenberg, A. J. M. *Organometallics* **1985**, *4*, 680.
(38) Mulliken, R. S. *J. Chem. Phys.* **1955**, *23*, 1831.
(39) (a) Gorelsky, S. I. *AOMix: Program for Molecular Orbital Analysis*, version 6.5; University of Ottawa, 2011; http://www.sg-chem.net/. (b) Gorelsky, S. I.; Lever, A. B. P. *J. Organomet. Chem.* **2001**, *635*, 187.
(40) (a) Brendler, E.; Wächtler, E.; Heine, T.; Zhechkov, L.; Langer, T.; Pöttgen, R.; Hill, A. F.; Wagler, J. *Angew. Chem., Int. Ed.* **2011**, *50*, 1. (b) Dostálová, R.; Dostál, L.; Ružička, A.; Jambor, R. *Organometallics* **2011**, *30*, 2405.
(41) Guy, J. J.; Sheldrick, G. M. *Acta Crystallogr., Sect. B: Struct. Crystallogr. Cryst. Chem* **1978**, *34*, 1722.
(42) Johnson, B. F. G.; Lewis, J.; Raithby, P. R.; Rosales, M. J. *J. Organomet. Chem.* **1983**, *259*, C9.
(43) Lloyd, B. R.; Puddephatt, R. J. *J. Am. Chem. Soc.* **1985**, *107*, 7785.
(44) Ohki, Y.; Uehara, N.; Suzuki, H. *Organometallics* **2003**, *22*, 59.
(45) Reichert, B. E.; Sheldrick, G. M. *Acta Crystallogr., Sect. B: Struct. Crystallogr. Cryst. Chem.* **1977**, *33*, 173.
(46) Wang, W.; Batchelor, R. J.; Einstein, F. W. B.; Lu, C.-Y.; Pomeroy, R. K. *Organometallics* **1993**, *12*, 3598.
(47) Khattar, R.; Johnson, B. F. G.; Lewis, J.; Raithby, P. R.; Rosales, M. J. *J. Chem. Soc., Dalton Trans.* **1990**, 2167.
(48) Wang, W.; Einstein, F. W.; Pomeroy, R. K. *Organometallics* **1994**, *13*, 1114.
(49) Sze-Yin Leung, K.; Wang, W.-T. *J. Chem. Soc., Dalton Trans.* **1999**, 2077.
(50) Rivera, A. V.; Sheldrick, G. M.; Hursthouse, M. B. *Acta Crystallogr., Sect. B: Struct. Crystallogr. Cryst. Chem.* **1978**, *34*, 3376.
(51) (a) Fachinetti, G.; Funaioli, T.; Zanazzi, P. F. *J. Organomet. Chem.* **1993**, *460*, C34. (b) Fumagalli, A.; Koetzle, T. F.; Takusagawa, F.; Chini, P.; Martinengo, S.; Heaton, B. T. *J. Am. Chem. Soc.* **1980**, *102*, 1740.
(52) Ruff, J. K.; White, R. P. Jr.; Dahl, L. F. *J. Am. Chem. Soc.* **1971**, *93*, 2159.
(53) (a) Bengtsson-Kloo, S.; Iapalucci, C. M.; Longoni, G.; Ulvenlund, S. *Inorg. Chem.* **1998**, *37*, 4335. (b) Pacchioni, G.; Rosch, N. *Inorg. Chem.* **1990**, *29*, 2901.
(54) (a) Albinati, A. *Inorg. Chim. Acta* **1977**, *22*, L31. (b) Albinati, A.; Carturan, G.; Musco, A. *Inorg. Chim. Acta* **1976**, *16*, L3. (c) Burrow, R. A.; Farrar, D. H.; Irwin, J. J. *Inorg. Chim. Acta* **1991**, *181*, 65. (d) Poverenov, E.; Gandelman, M.; Shimon, L. J. W.; Rozenberg, H.; Ben-David, Y.; Milstein, D. *Organometallics* **2005**, *24*, 1082.
(55) (a) Femoni, C.; Kaswalder, F.; Iapalucci, M. C.; Longoni, G.; Zacchini, S. *Eur. J. Inorg. Chem.* **2007**, 1483. (b) Femoni, C.; Kaswalder, F.; Iapalucci, M. C.; Longoni, G.; Mehlstaubl, M.; Zacchini, S. *Chem. Commun.* **2005**, 5769. (c) Femoni, C.; Iapalucci, M. C.; Longoni, G.; Lovato, T.; Stagni, S.; Zacchini, S. *Inorg. Chem.* **2010**, *49*, 5992. (d) Femoni, C.; Kaswalder, F.; Iapalucci, M. C.; Longoni, G.; Mehlstäubl, M.; Zacchini, S.; Ceriotti, A. *Angew. Chem., Int. Ed.* **2006**, *45*, 2060.
(56) Nagaki, D. A.; Lower, L. D.; Longoni, G.; Chini, P.; Dahl, L. F. *Organometallics* **1986**, *5*, 1764.
(57) (a) Mealli, C.; Ienco, A.; Proserpio, D. M. *Book of Abstracts of the XXXIII ICCC*, Florence, Italy, 1998; p 510. (b) Mealli, C.; Proserpio, D. M. *J. Chem. Educ.* **1990**, *67*, 399.
(58) Keller, E. *SCHAKAL99*; University of Freiburg: Germany, 1999.
(59) Sheldrick, G. M. *SADABS, Program for empirical absorption correction*; University of Göttingen: Göttingen, Germany, 1996.
(60) Sheldrick, G. M. *Acta Crystallogr.* **2008**, *A64*, 112.
(61) Frisch, M. J.et al. *Gaussian 09*, revision B.01; Gaussian, Inc.: Wallingford CT, 2010.
(62) Dolg, M.; Stoll, H.; Preuss, H.; Pitzer, R. M. *J. Phys. Chem.* **1993**, *97*, 5852.
(63) (a) Hoffmann, R.; Lipscomb, N. W. *J. Chem. Phys.* **1962**, *36*, 2872. (b) Hoffmann, R.; Lipscomb, W. N. *J. Chem. Phys.* **1962**, *37*, 3489.